Supporting Information for:

On the Mechanism of Ni(II)-Promoted Michael-Type Hydroamination of Acrylonitrile and Its Substituted Derivatives

Sébastien Lapointe and Davit Zargarian[†]

[†] Département de chimie, Université de Montréal, Montréal (Québec), Canada H3C 3J6

Table S1 Crystal Data, Collection, and Refinement Parameters for complexes **7, 9** and **10**

	7	**9**	**10**
chemical formula	$C_{23}H_{36}NNiO_4P_2,CF_3O_3S$	$C_{29}H_{40}NNiO_4P_2,CF_3O_3S$	$C_{28}H_{40}NNiO_3P_2,C_9H_7N,CF_3O_3S$
crystal colour	yellow	yellow	yellow
***Fw*; *F*(000)**	660.25; 688	736.34; 1536	838.00; 1753
***T* (K)**	100	100	100
wavelength (Å)	1.34139	1.54178	1.34139
space group	P -1	P 1 21/n 1	P 1 21/n 1
***a* (Å)**	8.1449(4)	7.88780(8)	9.2880(6)
***b* (Å)**	10.6295(5)	10.89270(11)	35.220(2)
***c* (Å)**	18.1924(8)	40.6954(4)	12.8458(8)
α (deg)	78.203(2)	90	90
β (deg)	77.454(2)	91.8910(5)	102.689(4)
γ (deg)	89.556(2)	90	90
Z	2	4	4
***V* (Å^3)**	1503.84(12)	3494.62(6)	4099.5(5)
ρ_{calcd} (g·cm^{-3})	1.458	1.400	1.358
μ (mm^{-1})	5.020	2.748	3.755
θ range (deg); completeness	2.213 − 60.849; 1.000	2.172 − 71.668; 0.999	2.183 − 60.730; 0.999
collected reflections; R_σ	45548; 0.0342	92637; 0.0099	61357; 0.0307
unique reflections; R_{int}	45548; 0.0550	92637; 0.0250	61357; 0.0463
R1[a]; wR2[b] [I > 2σ(I)]	0.0370; 0.0946	0.0316; 0.0821	0.0477; 0.1155
R1; wR2 [all data]	0.0481; 0.1008	0.0320; 0.0824	0.0518; 0.1178
GOF	1.044	1.124	1.108
largest diff peak and hole	0.646 and -0.375	0.387 and -0.272	1.524 and -0.427

a) $R_1=\Sigma(||F_o|-|F_c||)/\Sigma|F_o|$ b) $wR_2=\{\Sigma[w(F_o^2-F_c^2)^2]/\Sigma[w(F_o^2)^2]\}^{½}$

Table S2 Crystal Data, Collection, and Refinement Parameters for complexes **11** and **12**

	11	**12**
chemical formula	$C_{18}H_{34}NNiO_2P_2,CF_3O_3S$	$C_{20}H_{36}NNiO_4P_2,CF_3O_3S$
crystal colour	yellow	colourless
***Fw*; *F*(000)**	566.18; 592	624.22; 652
***T* (K)**	100	100
wavelength (Å)	1.34139	1.34139
space group	P -1	P -1
***a* (Å)**	7.5940(3)	7.5293(3)
***b* (Å)**	12.8525(5)	11.2755(5)
c (Å)	14.7380(5)	17.2859(7)
α (deg)	76.845(2)	84.276(2)
β (deg)	76.375(2)	88.649(2)
γ (deg)	73.105(2)	87.103(2)
Z	2	2
***V* (Å^3)**	1317.91(9)	1458.08(11)
ρ_{calcd} (g·cm^{-3})	1.427	1.422
μ (mm^{-1})	5.625	5.154
θ range (deg); completeness	2.724 − 60.788; 1.000	2.235 − 60.764; 0.998
collected reflections; R_σ	38553; 0.0318	42662; 0.0316
unique reflections; R_{int}	38553; 0.0486	42662; 0.0505
R1[a]; wR2[b] [I > 2σ(I)]	0.0298; 0.0776	0.0327; 0.0885
R1; wR2 [all data]	0.0337; 0.0798	0.0361; 0.0903
GOF	1.067	1.078
largest diff peak and hole	0.543 and -0.294	0.609 and -0.234

a) $R_1=\Sigma(||F_o|-|F_c||)/\Sigma|F_o|$ b) $wR_2=\{\Sigma[w(F_o^2-F_c^2)^2]/\Sigma[w(F_o^2)^2]\}^{1/2}$

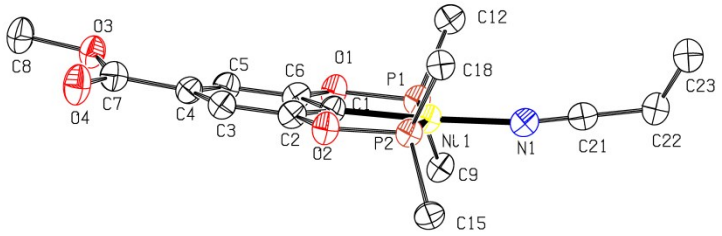

Figure S1 Side view of the molecular diagram for complex **7**.

Thermal ellipsoids are shown at the 50% probability level. *P*-substituents and hydrogens are omitted for clarity.

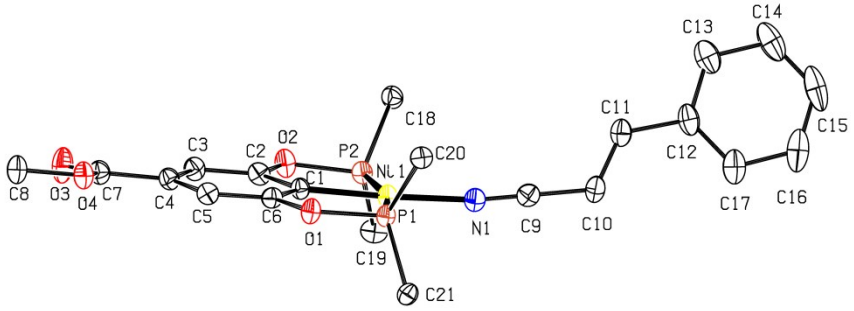

Figure S2 Side view of the molecular diagram for complex **9**.

Thermal ellipsoids are shown at the 50% probability level. *P*-substituents and hydrogens are omitted for clarity

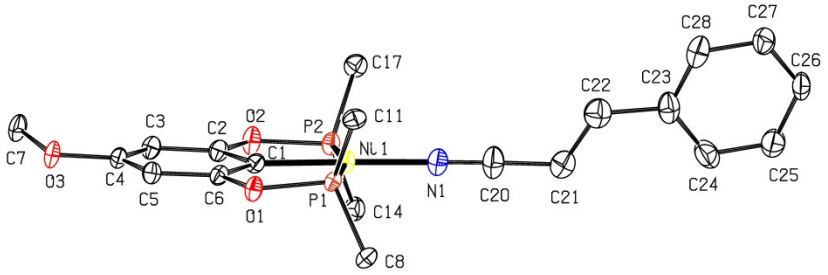

Figure S3 Side view of the molecular diagram for complex **10**.

Thermal ellipsoids are shown at the 50% probability level. *P*-substituents and hydrogens are omitted for clarity

Details of the diffraction studies

Crystals of compound **7** were obtained by slow evaporation of a concentrated THF solution at r.t. Crystals of compound **9** and **10** were obtained by slow evaporation of a concentrated dichloromethane solution at r.t. Crystals of compound **11** and **12** were obtained by slow evaporation of a concentrated acetone solution at r.t. The crystallographic data for all complexes were collected on a Bruker Venture Metaljet equipped with a Metal Jet source, an Helios MX Mirror Optics monochromator and a Bruker Photon 100 CMOS Detector. Cell refinement and data reduction were done using the ShelXL routine version July 2014.[1] An empirical absorption correction, based on the multiple measurements of equivalent reflections, was applied. The space group was confirmed by ShelXT [2] routine in the program OLEX2.[3] The structures were solved by direct methods (ShelXT) and refined by full-matrix least-squares and difference Fourier techniques with OLEX2.[3] All non-hydrogen atoms were refined with anisotropic displacement parameters. Hydrogen atoms were set in calculated positions and refined as riding atoms with a common thermal parameter

NMR Analysis

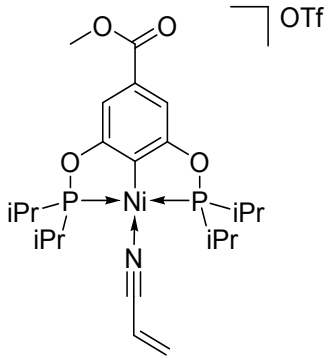

Figure S4 Representation of complex [{2,6-(iPr$_2$PO)$_2$-4-(CO_2Me)C_6H_2}Ni(NCCH=CH_2)][OSO_2CF_3] (**7**)

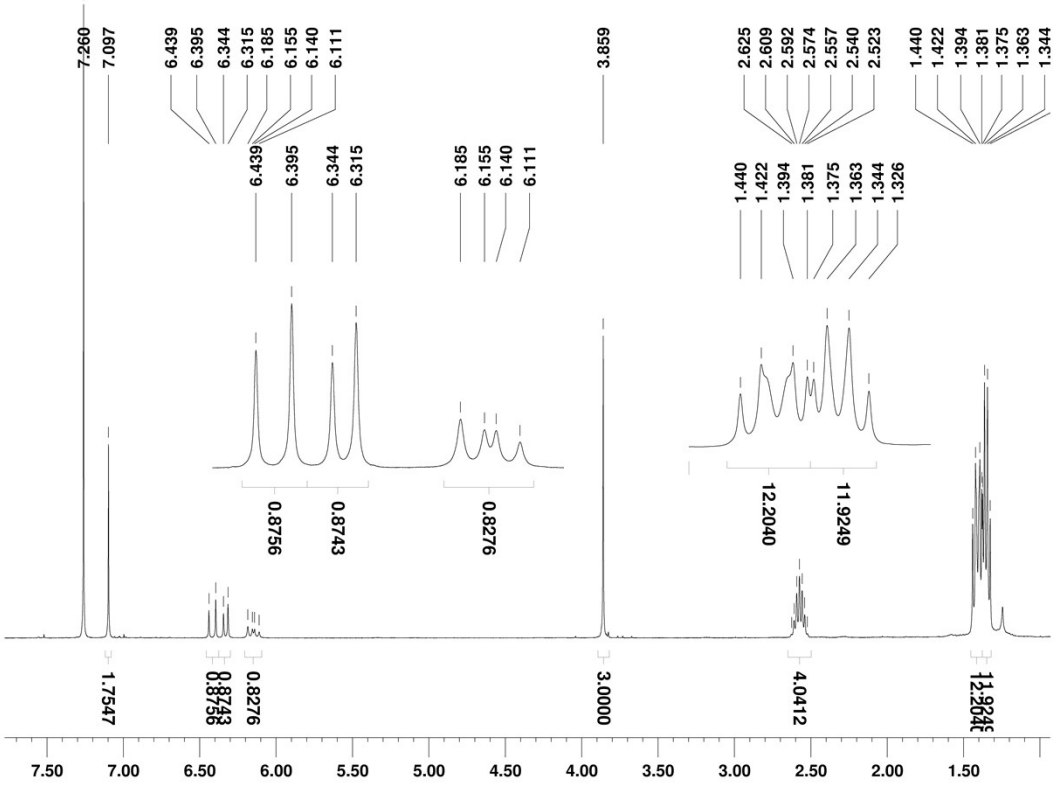

Figure S5 ^{1}H NMR spectra (400 MHz) of complex **7** in $CDCl_3$

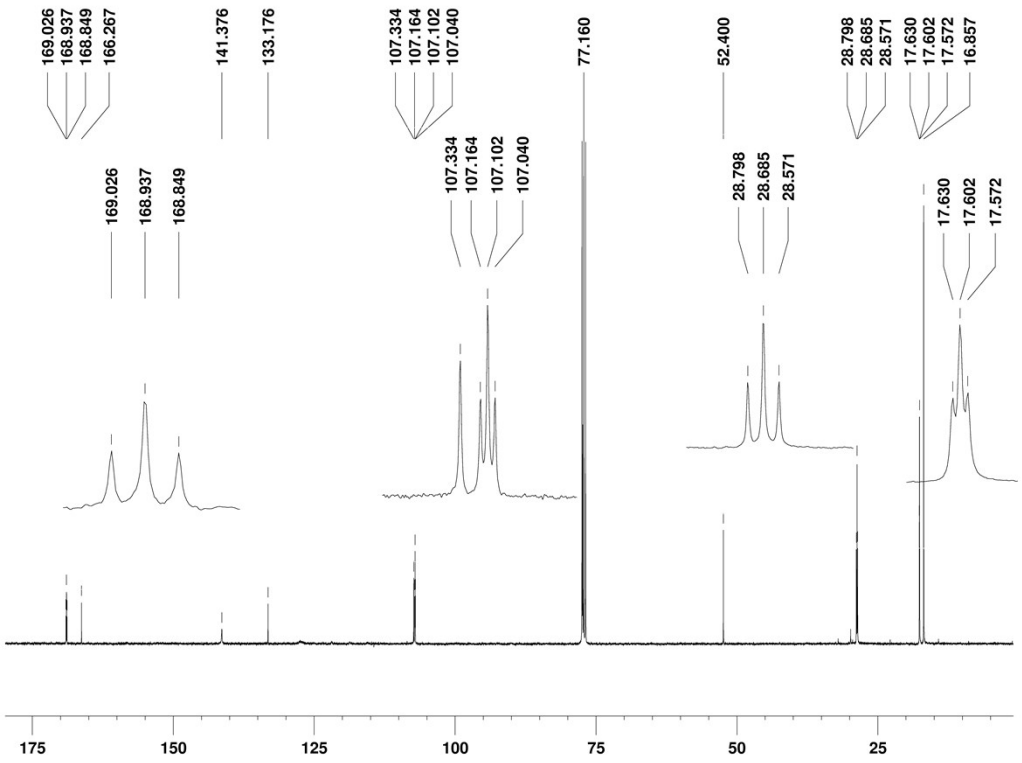

Figure S6 $^{13}C\{^{1}H\}$ NMR spectra (101 MHz) of complex **7** in $CDCl_3$

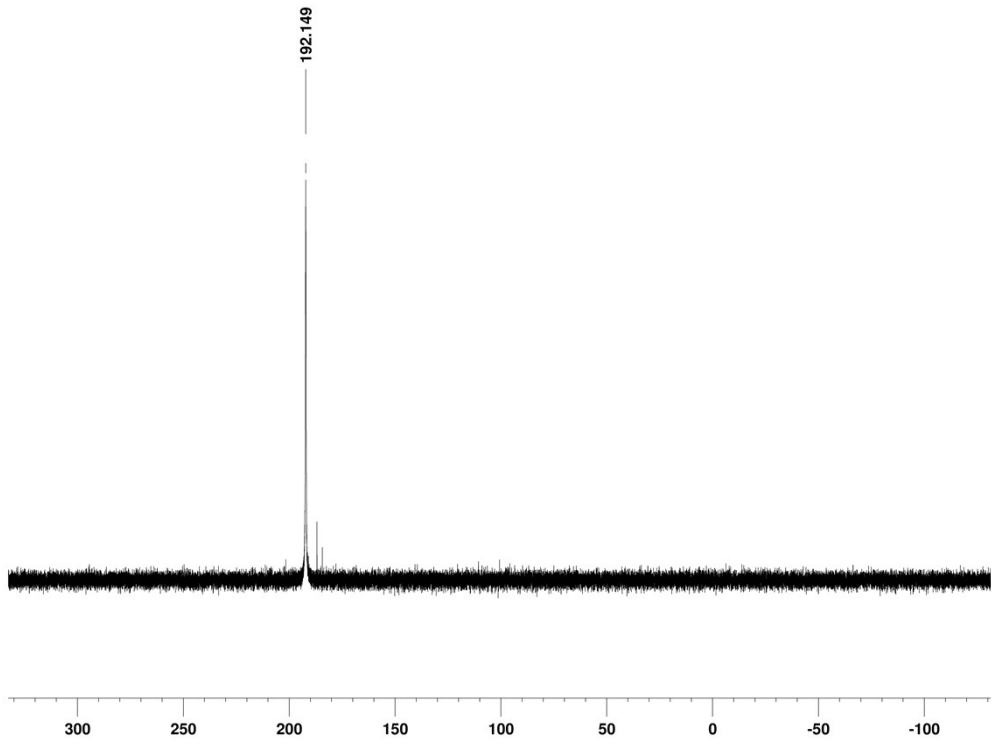

Figure S7 $^{31}P\{^{1}H\}$ NMR spectra (162 MHz) of complex **7** in $CDCl_3$

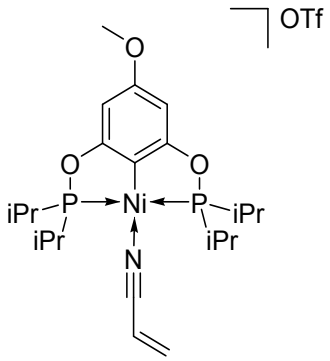

Figure S8 Representation of complex [{2,6-(iPr$_2$PO)$_2$-4-(OMe)C$_6$H$_2$}Ni(NCCH=CH$_2$)][OSO$_2$CF-$_3$] (**8**)

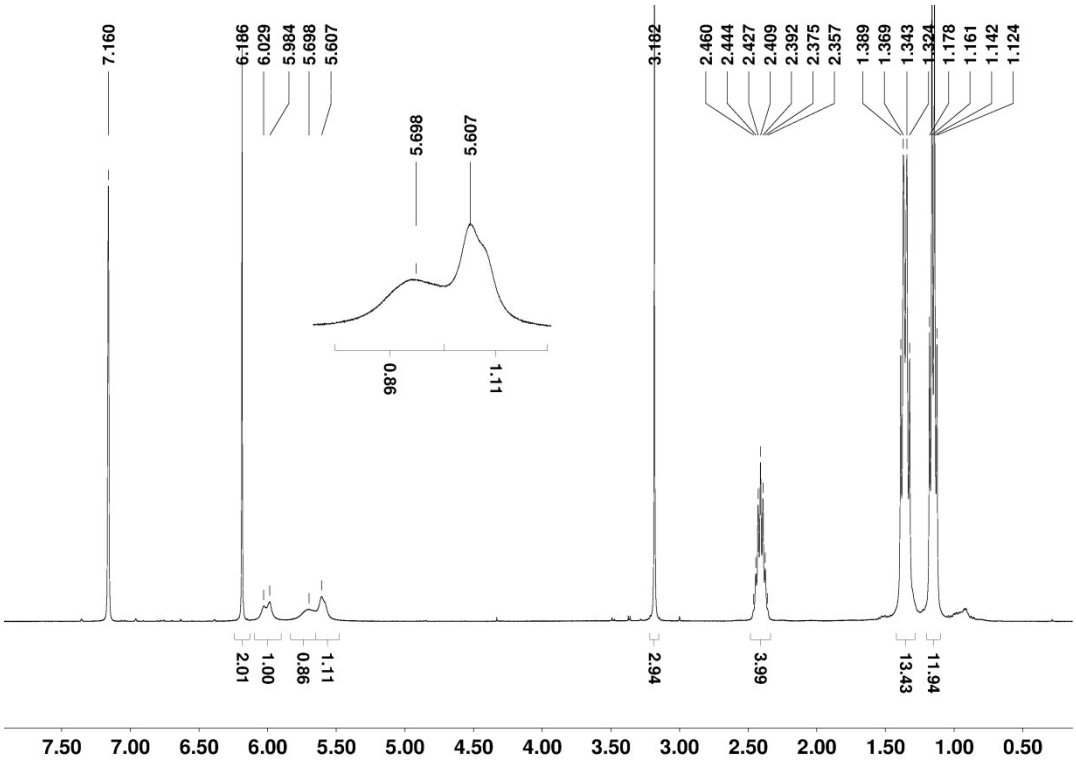

Figure S9 ^{1}H NMR spectra (500 MHz) of complex **8** in C$_6$D$_6$

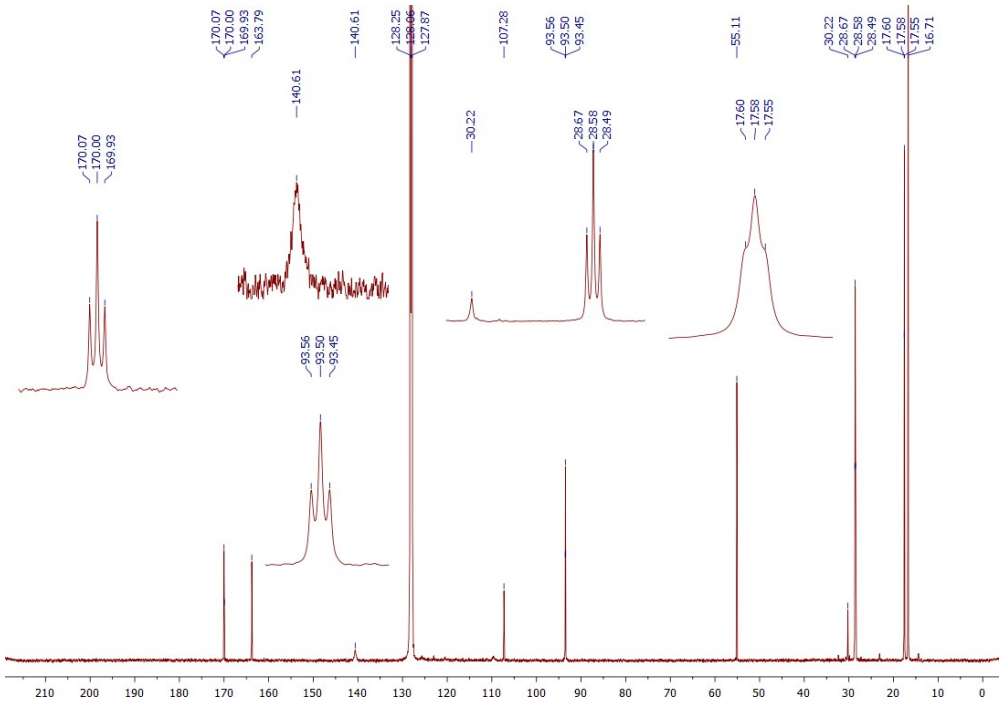

Figure S10 $^{13}C\{^{1}H\}$ NMR spectra (125 MHz) of complex **8** in C_6D_6

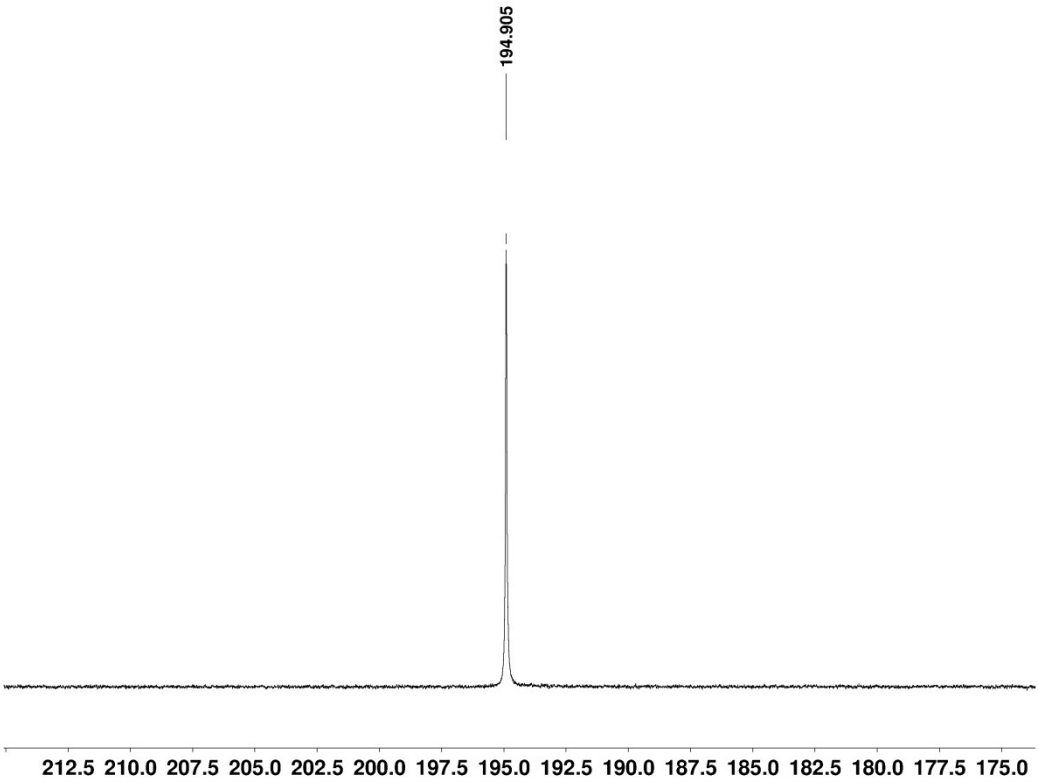

Figure S11 $^{31}P\{^{1}H\}$ NMR spectra (162 MHz) of complex **8** in C_6D_6

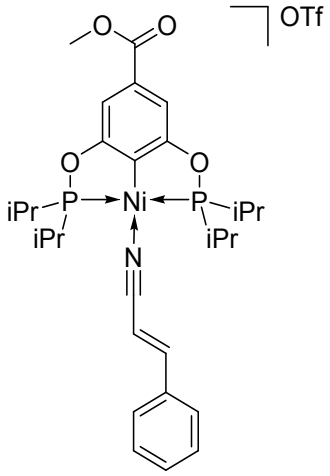

Figure S12 Representation of complex [{2,6-(iPr$_2$PO)$_2$-4-(CO_2Me)C_6H_2}Ni(NCCH=CHPh)][OSO_2CF_3] (**9**)

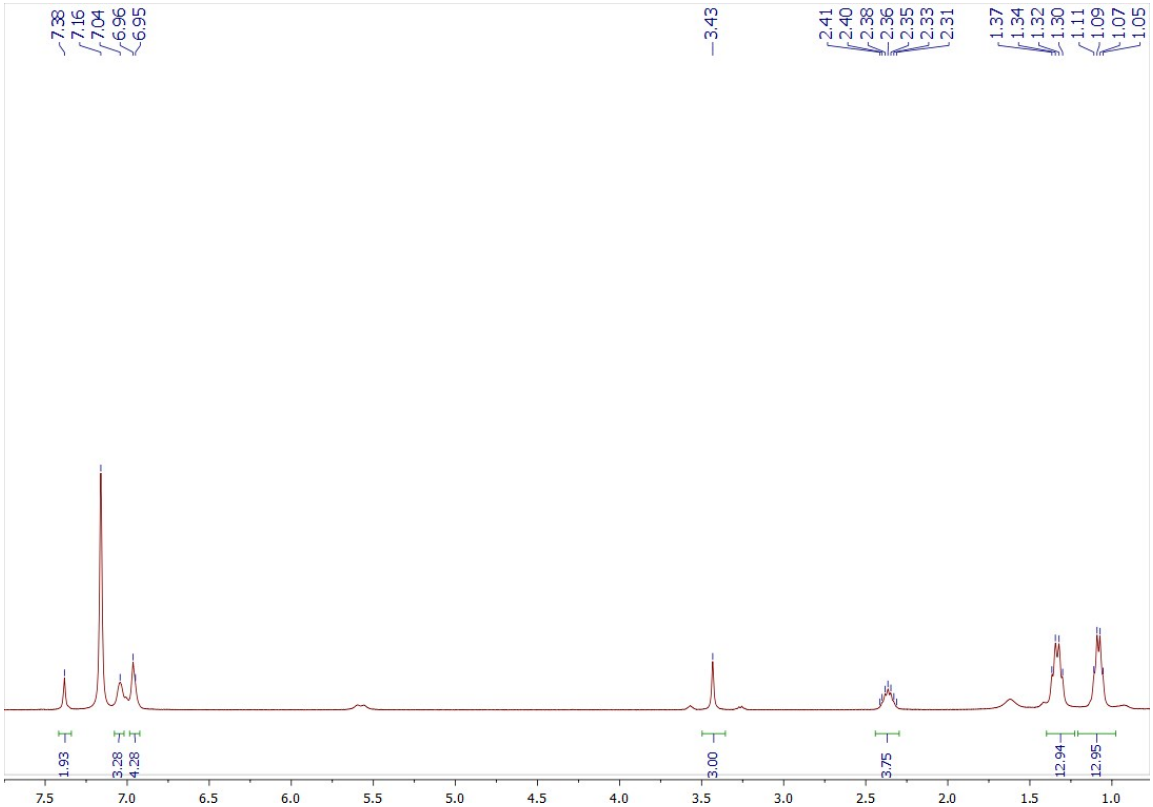

Figure S13 ^{1}H NMR spectra (400 MHz) of complex **9** in C_6D_6

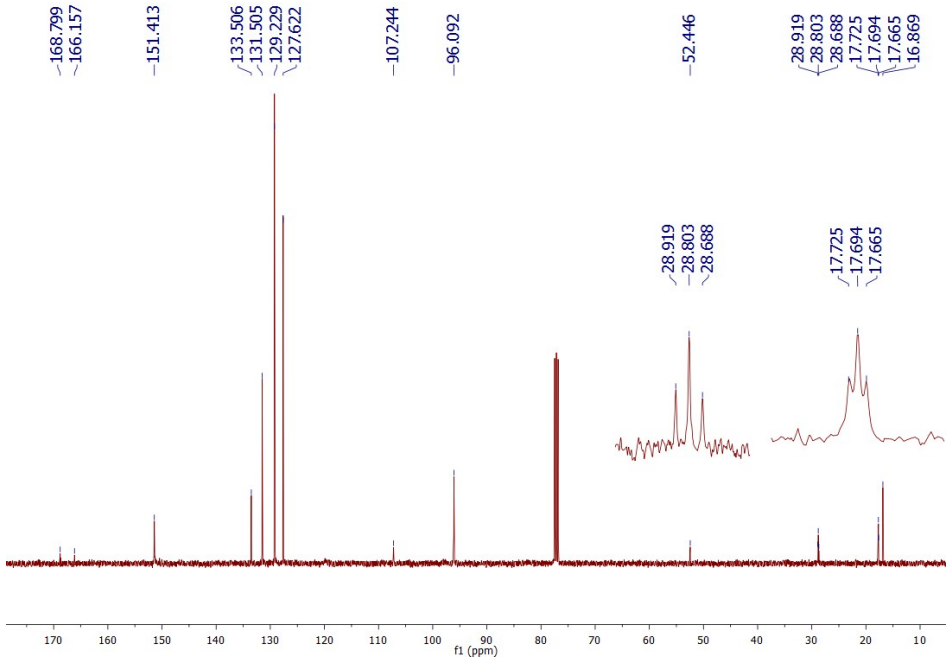

Figure S14 $^{13}C\{^{1}H\}$ NMR spectra (MHz) of complex **9** in $CDCl_3$

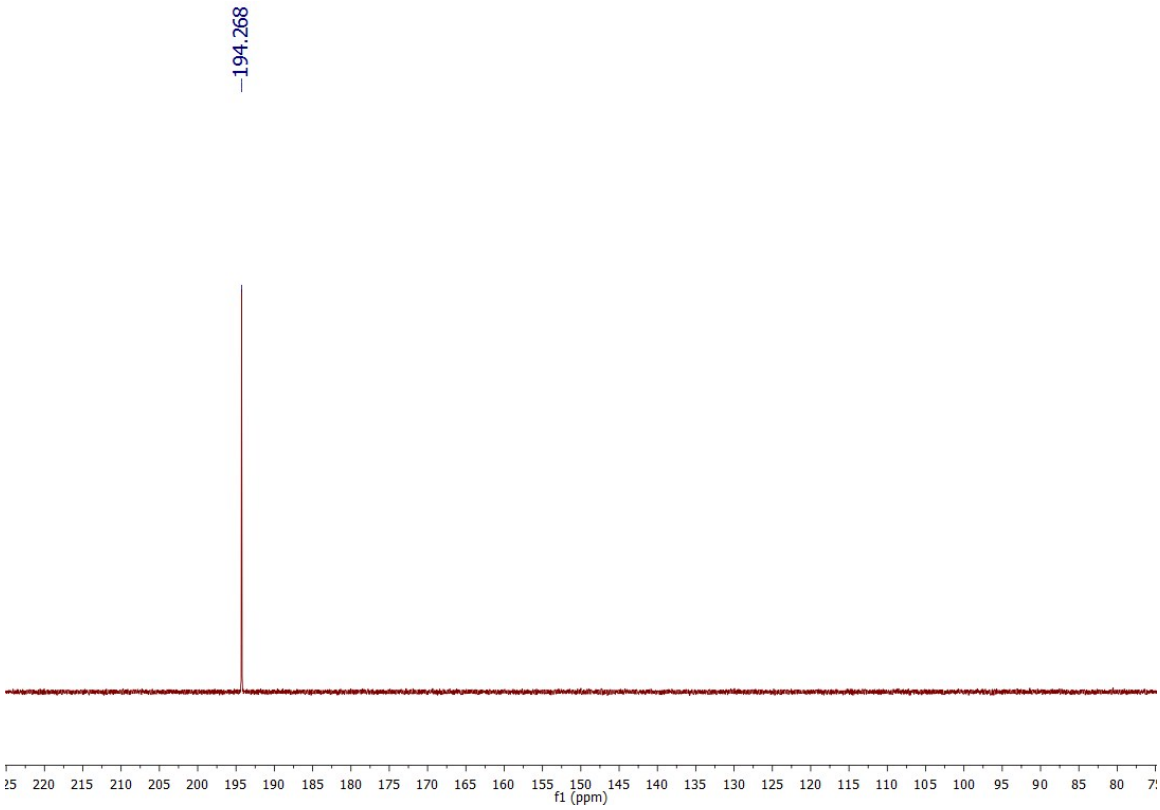

Figure S15 $^{31}P\{^{1}H\}$ NMR spectra (MHz) of complex **9** in $CDCl_3$

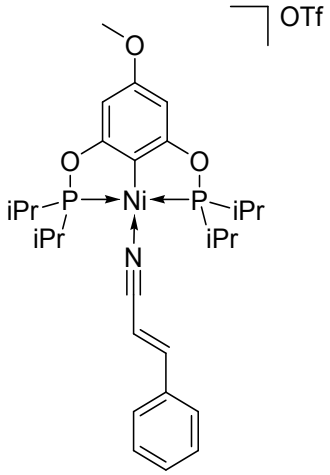

Figure S16 Representation of complex [{2,6-(iPr$_2$PO)$_2$-4-(OMe)C$_6$H$_2$}Ni(NCCH=CHPh)][OSO$_2$CF$_3$]. (NCCH=CHPh) (**10**)

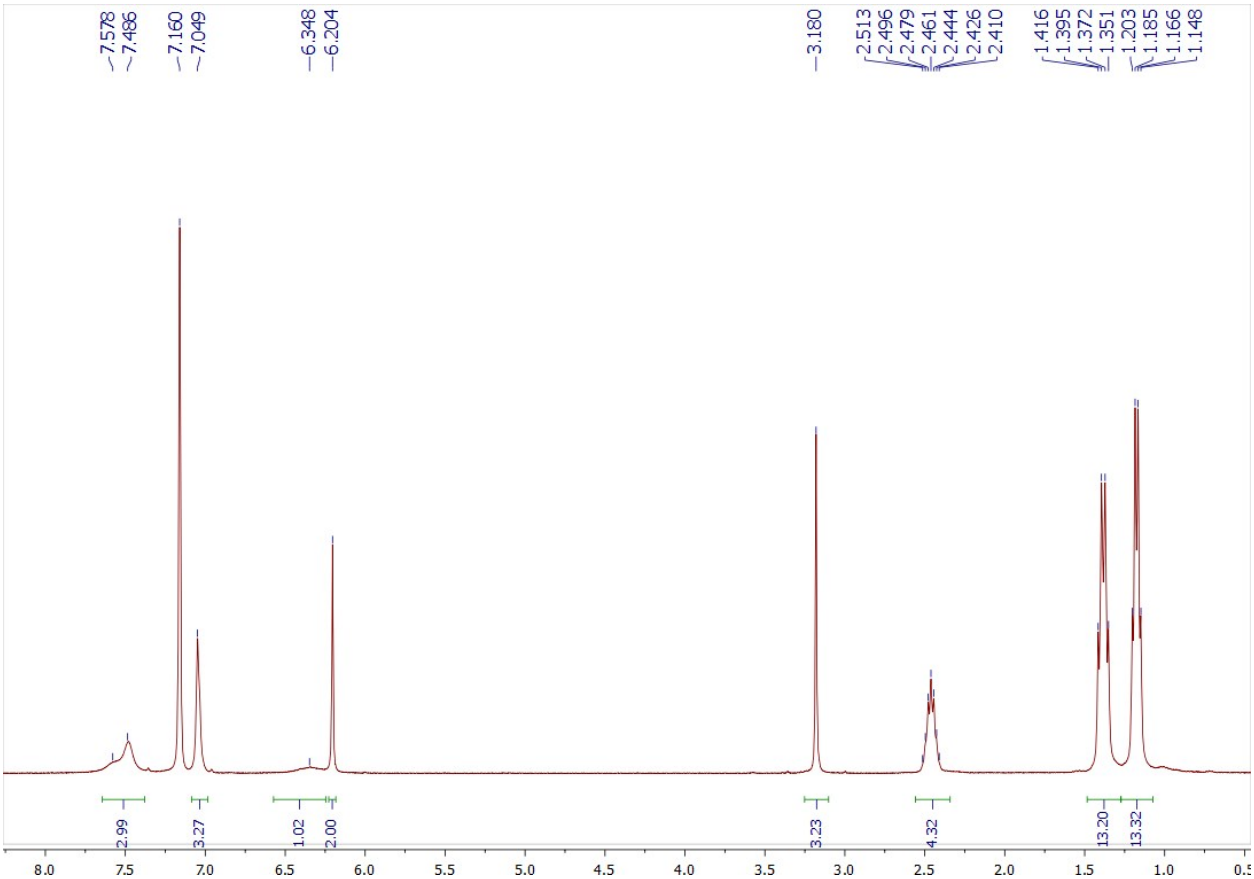

Figure S17 ^{1}H NMR spectra (400 MHz) of complex **10** in C$_6$D$_6$

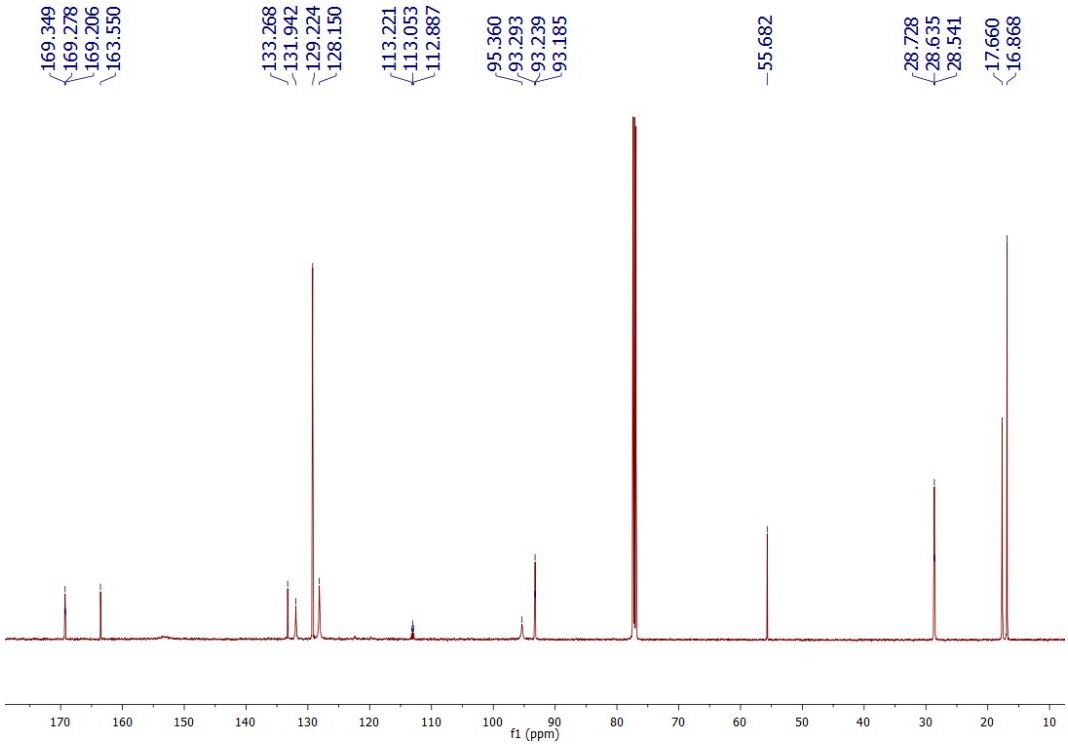

Figure S18 $^{13}C\{^{1}H\}$ NMR spectra (101 MHz) of complex **10** in $CDCl_3$

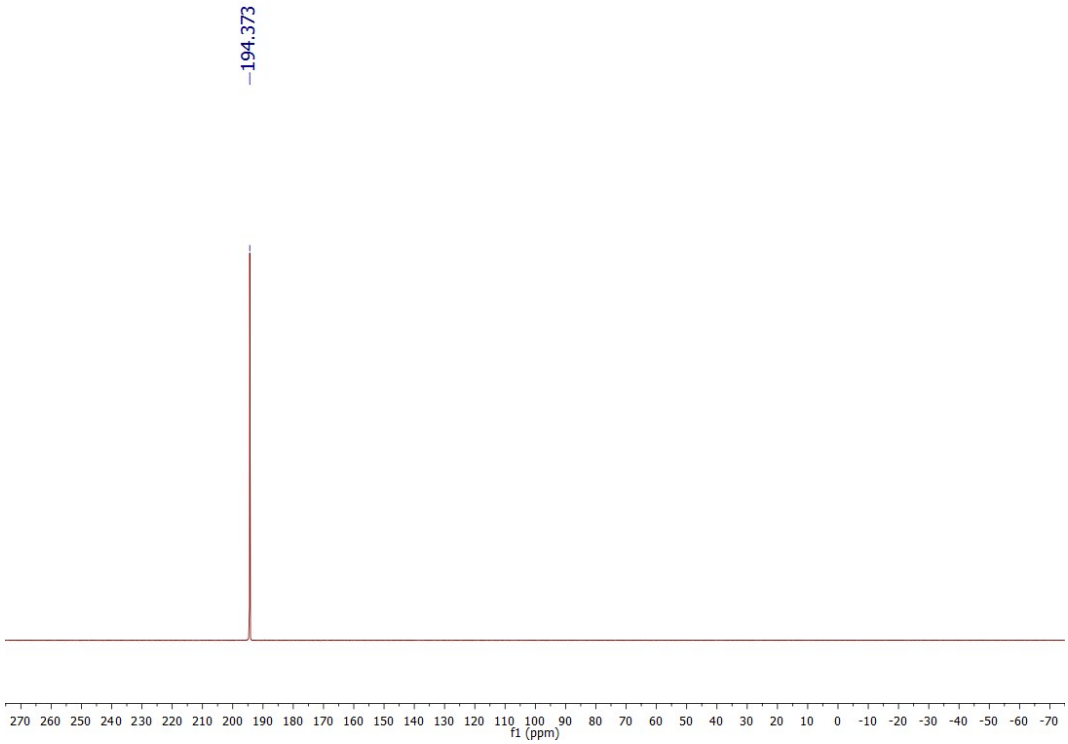

Figure S19 $^{31}P\{^{1}H\}$ NMR spectra (162 MHz) of complex **10** in $CDCl_3$

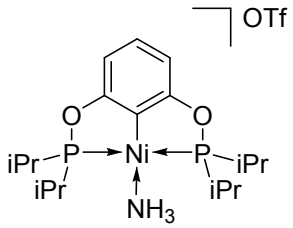

Figure S20 Representation of complex [{2,6-(iPr$_2$PO)$_2$C$_6$H$_3$}Ni(NH$_3$)][OSO$_2$CF$_3$] (**11**)

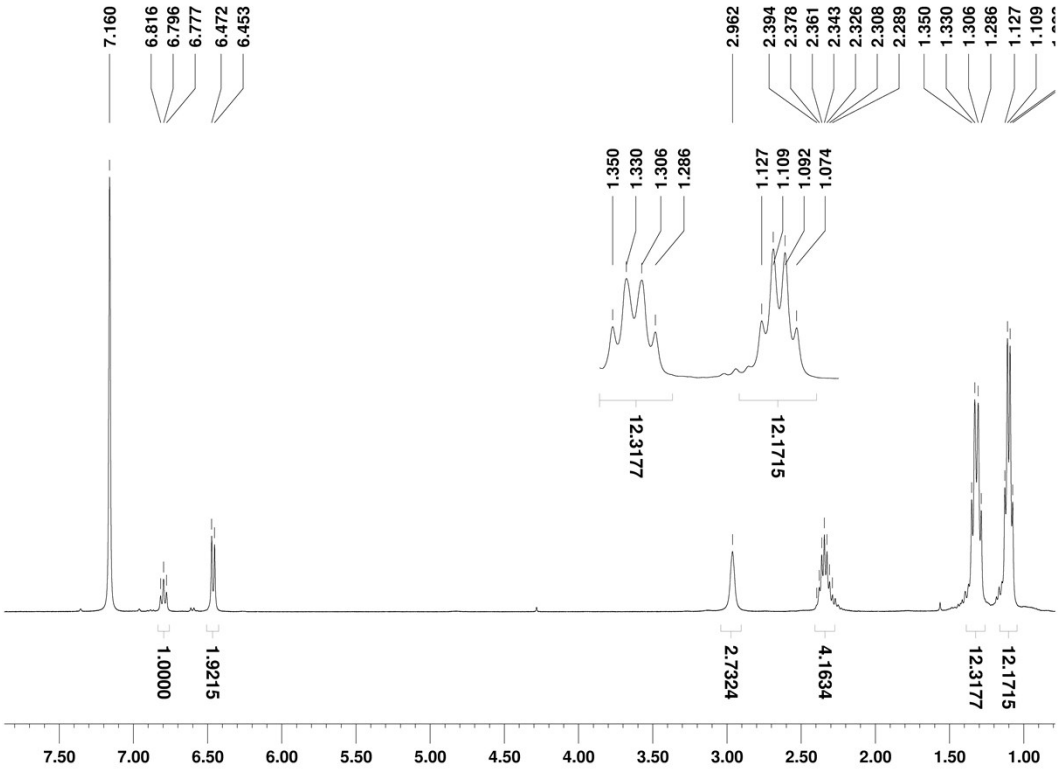

Figure S21 ^{1}H NMR spectra (400 MHz) of complex **11** in C$_6$D$_6$

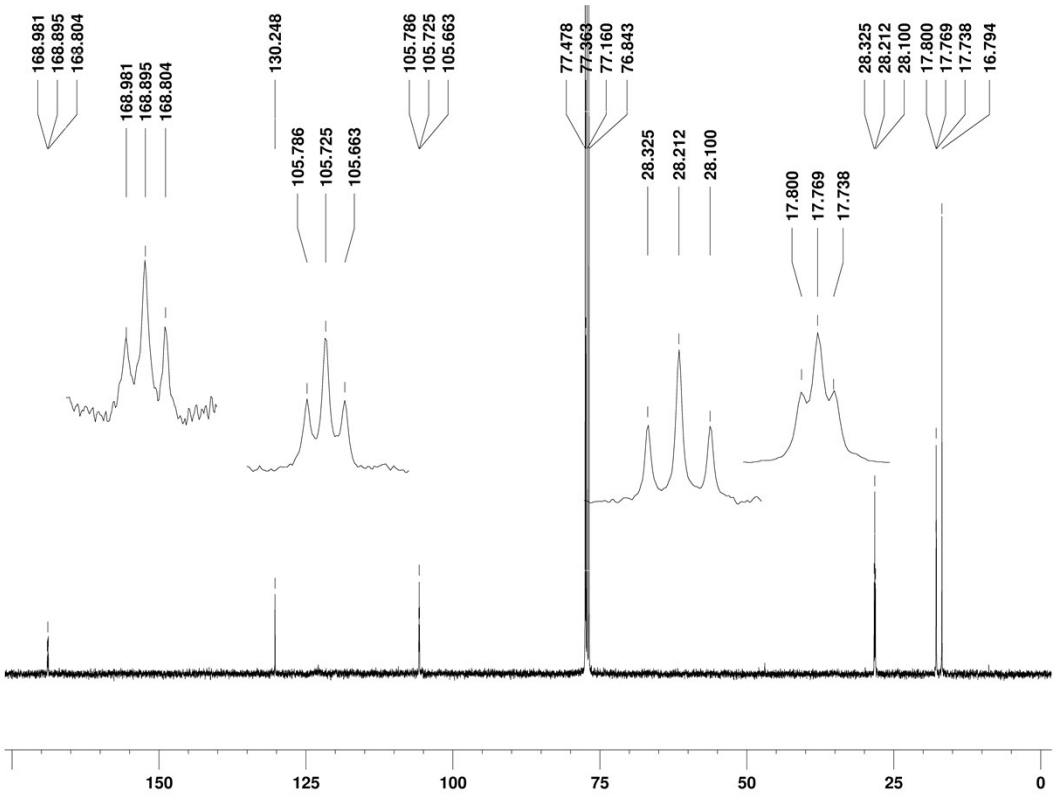

Figure S22 $^{13}C\{^{1}H\}$ NMR spectra (101 MHz) of complex **11** in $CDCl_3$

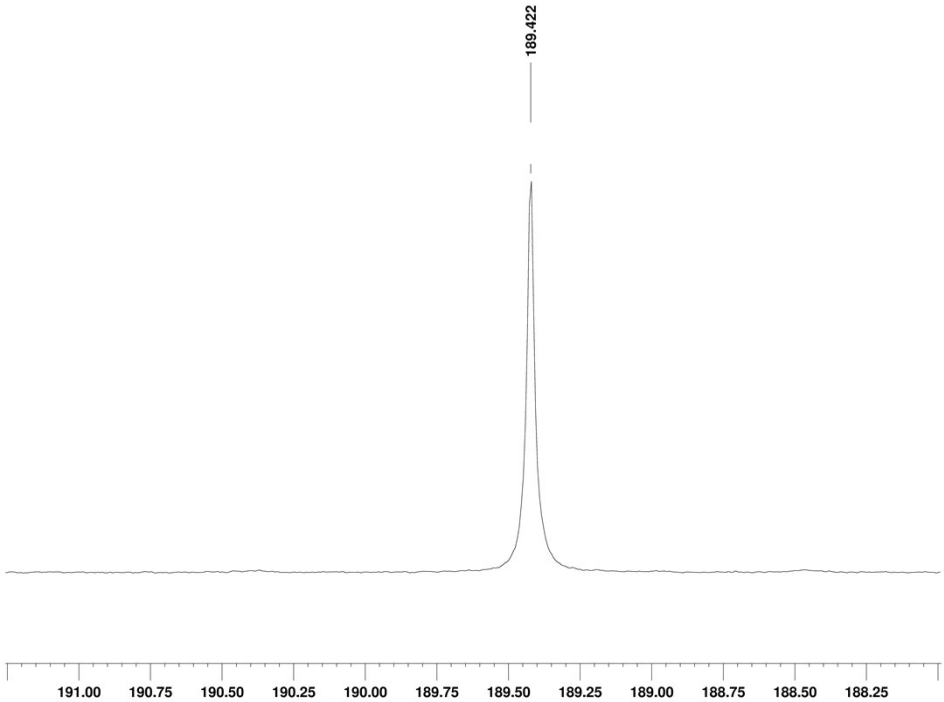

Figure S23 $^{31}P\{^{1}H\}$ NMR spectra (162 MHz) of complex **11** in C_6D_6

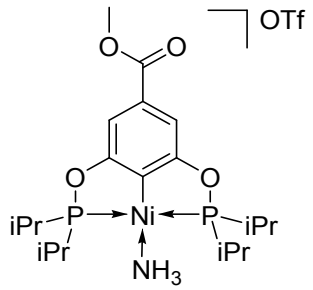

Figure S24 Representation of complex [{2,6-(*i*Pr$_2$PO)$_2$-4-(CO$_2$Me)C$_6$H$_2$}Ni(NH$_3$)][OSO$_2$CF$_3$] (**12**)

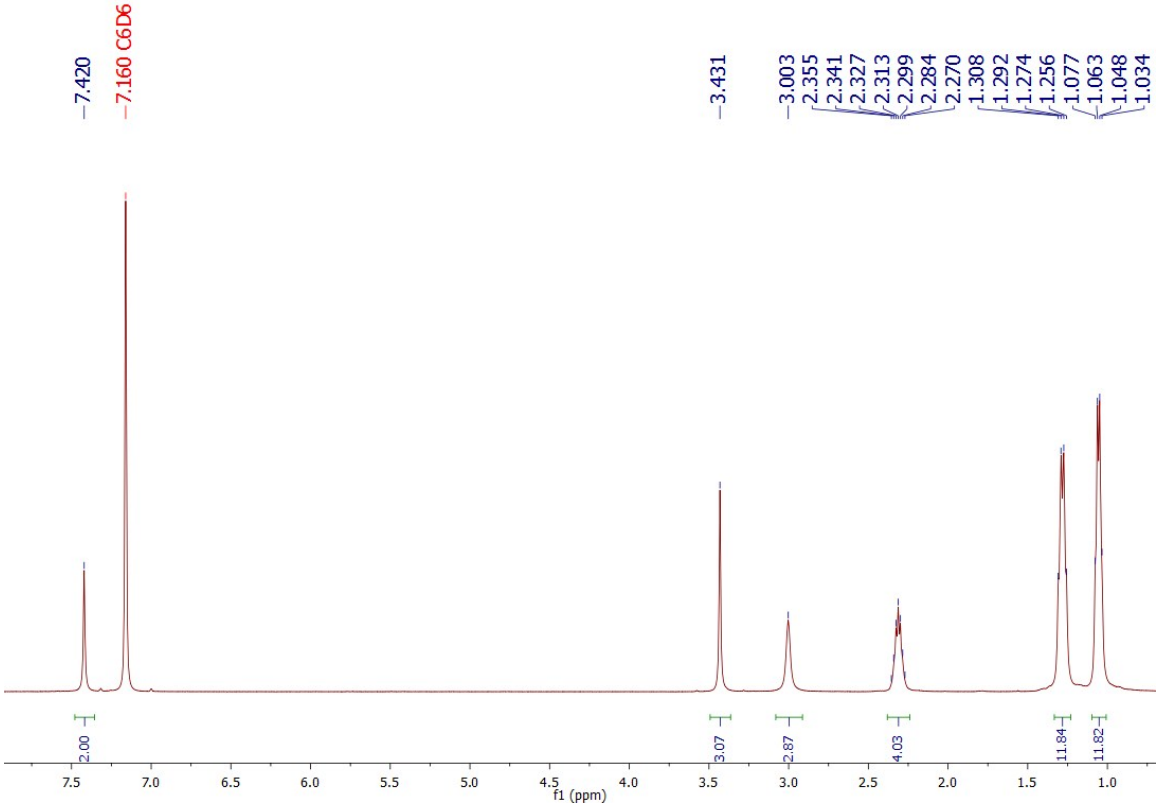

Figure S25 ^{1}H NMR spectra (500 MHz) of complex **12** in C$_6$D$_6$

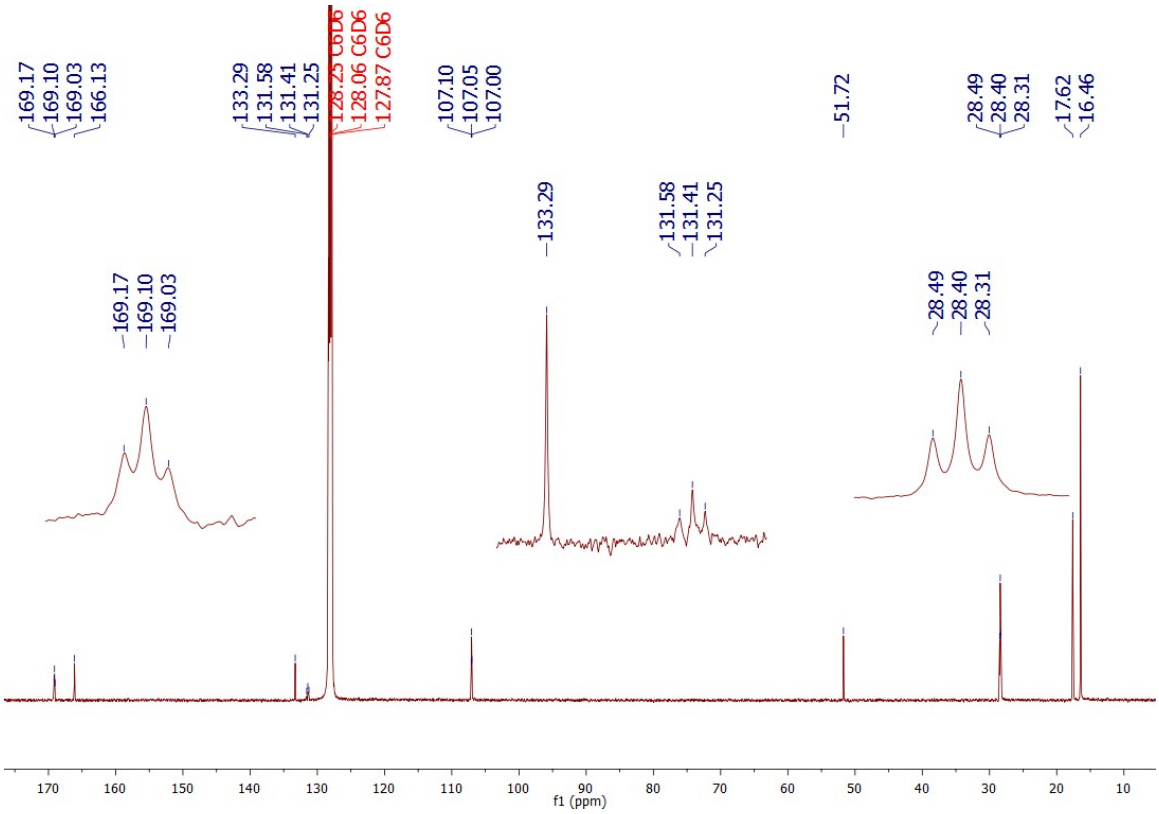

Figure S26 $^{13}C\{^{1}H\}$ NMR spectra (125 MHz) of complex **12** in C_6D_6

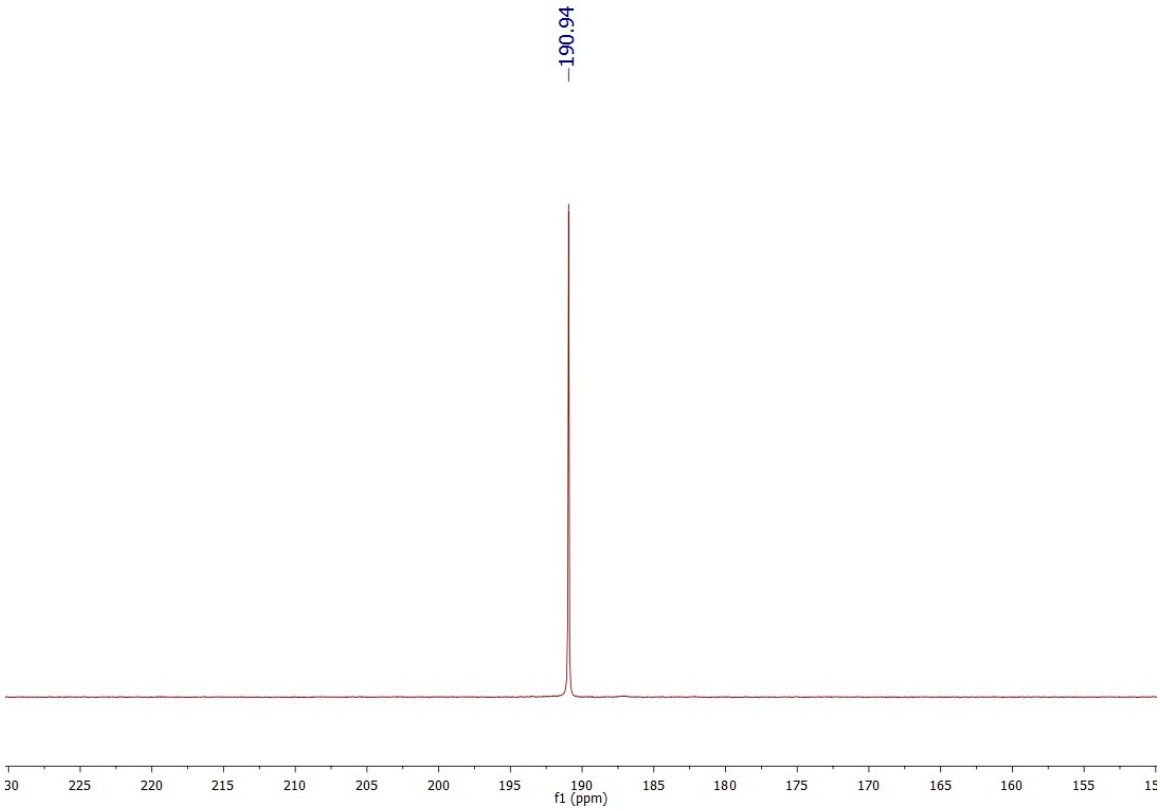

Figure S27 $^{31}P\{^{1}H\}$ NMR spectra (202 MHz) of complex **12** in C_6D_6

Catalytic Tests

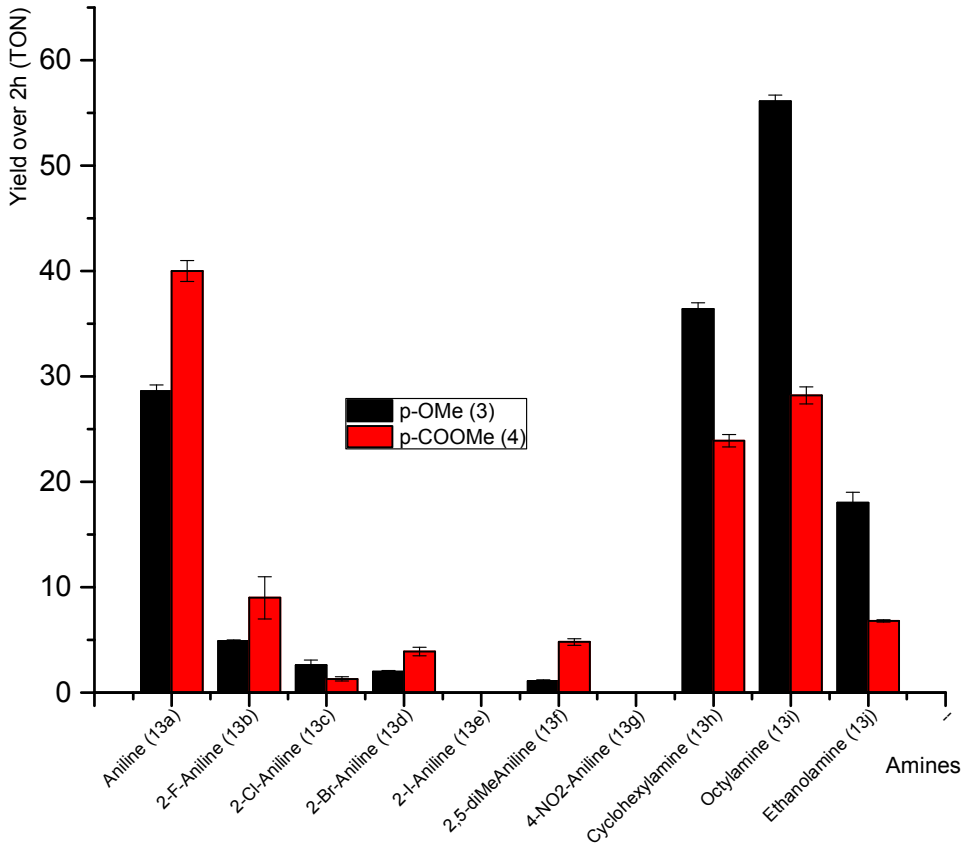

Figure S28 Plot of the yield (TON) for the hydroamination of crotonitrile (14a) catalyzed by **3** and **4** for the mono-addition product over 2 h.

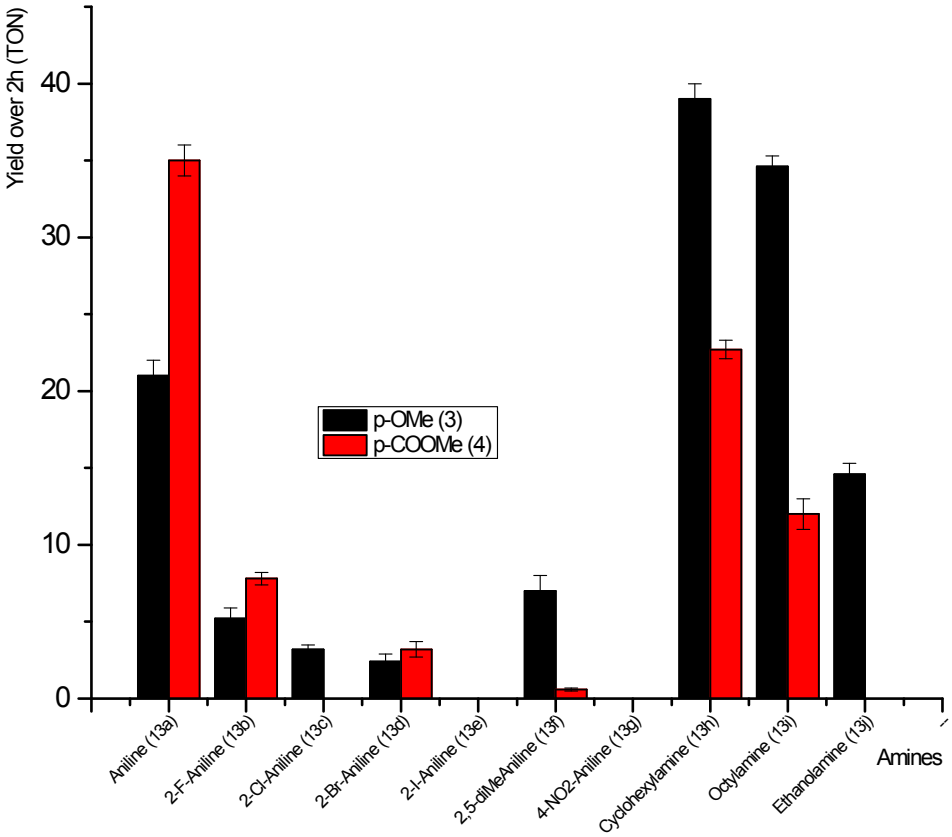

Figure S29 Plot of the yield (TON) for the hydroamination of methacrylonitrile (14b) catalyzed by **3** and **4** for the mono-addition product over 2 h.

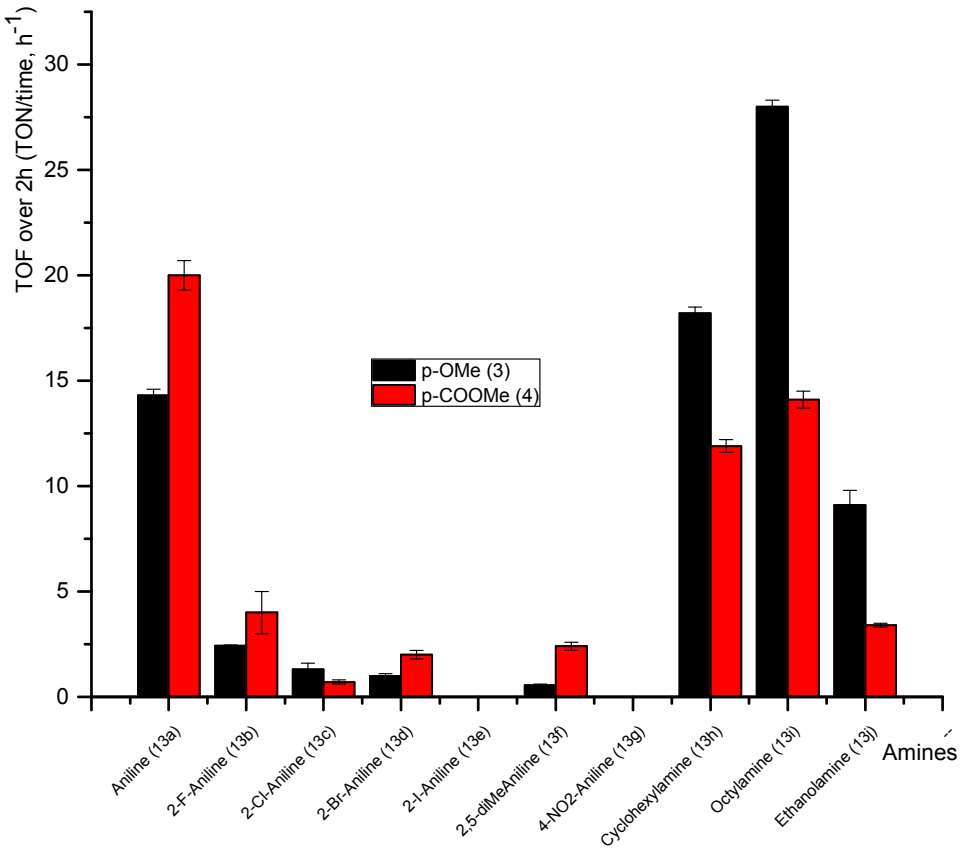

Figure S30 Plot of the TOF (TON/time, h^{-1}) for the hydroamination of crotonitrile (14a) catalyzed by **3** and **4** for the mono-addition product over 2 h.

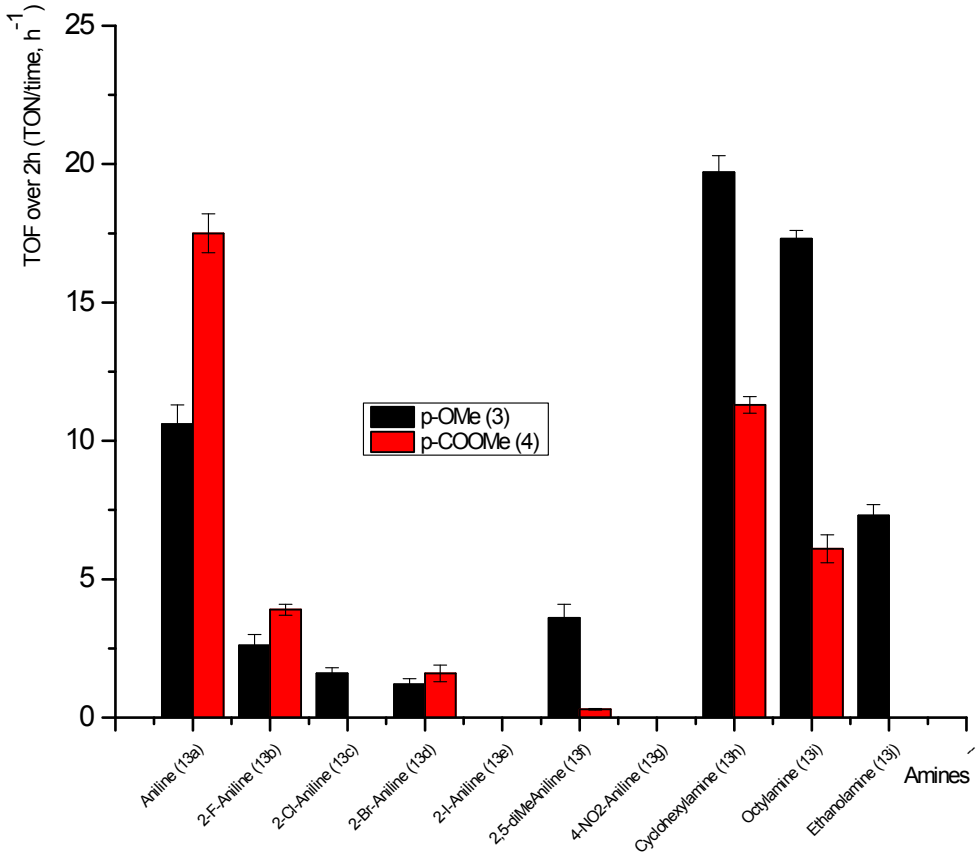

Figure S31 Plot of the TOF (TON/time, h^{-1}) for the hydroamination of methacrylonitrile (14b) catalyzed by **3** and **4** for the mono-addition product over 2 h

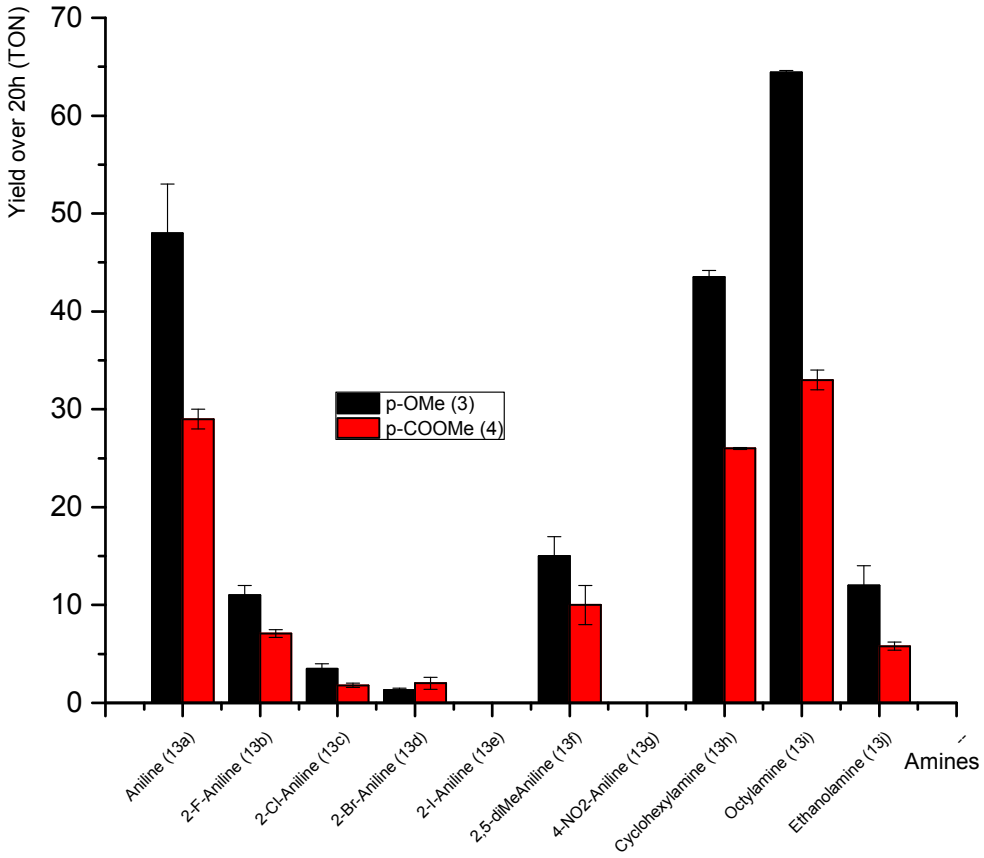

Figure S32 Plot of the yield (TON) for the hydroamination of crotonitrile (14a) catalyzed by **3** and **4** for the mono-addition product over 20 h.

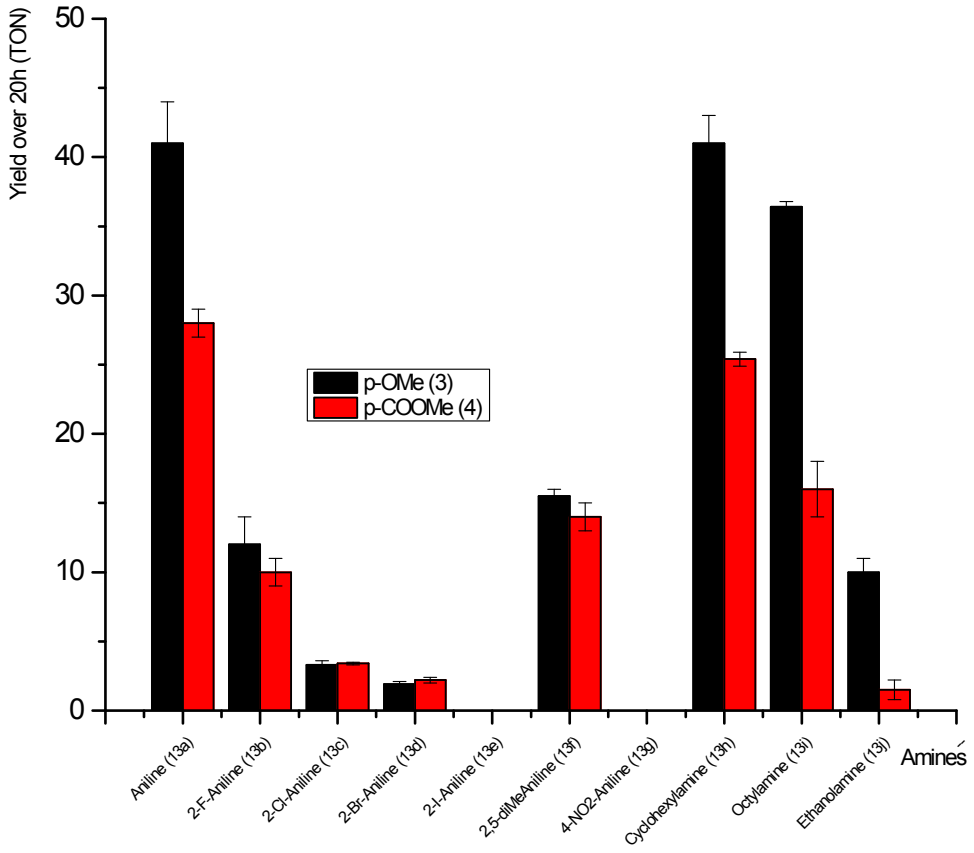

Figure S33 Plot of the yield (TON) for the hydroamination of methacrylonitrile (14b) catalyzed by **3** and **4** for the mono-addition product over 20 h.

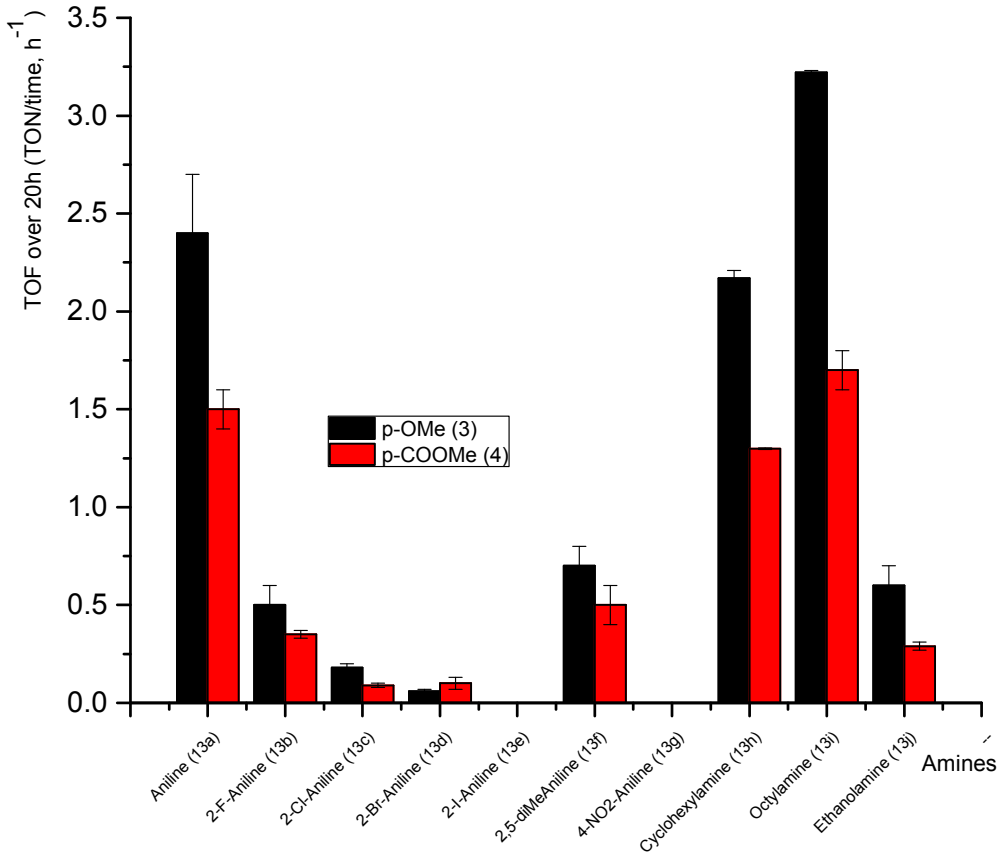

Figure S34 Plot of the TOF (TON/time, h^{-1}) for the hydroamination of crotonitrile (14a) catalyzed by **3** and **4** for the mono-addition product over 20 h

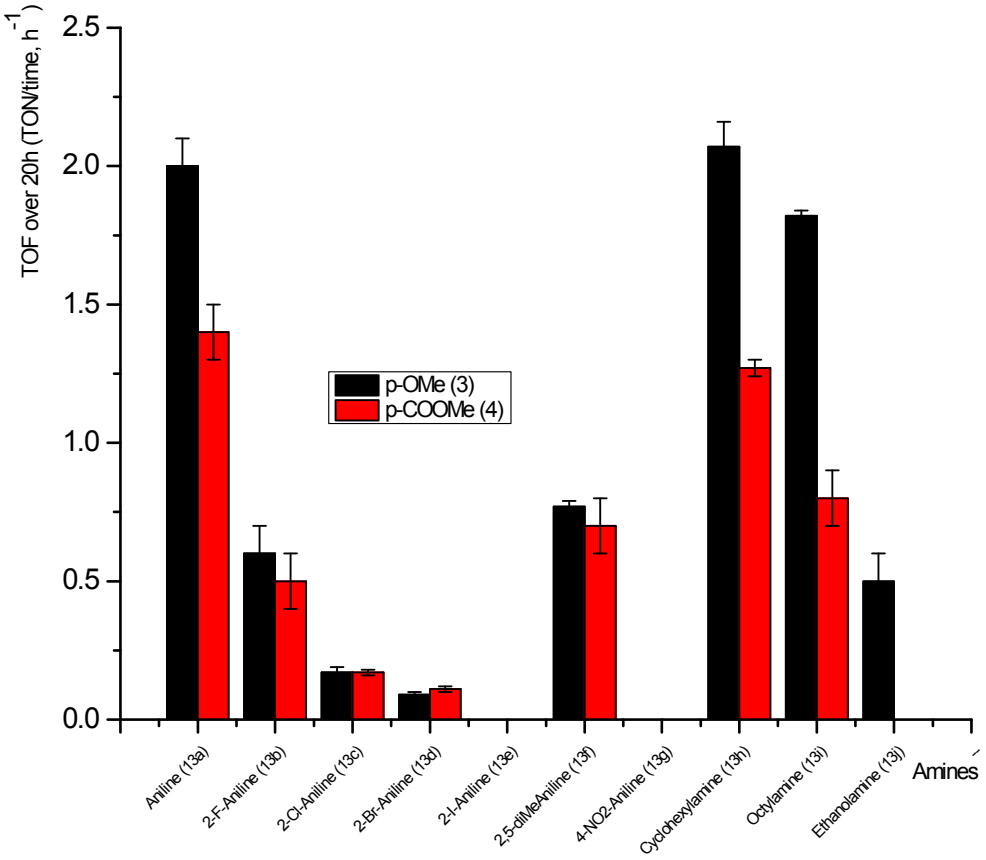

Figure S35 Plot of the TOF (TON/time, h^{-1}) for the hydroamination of methacrylonitrile (14b) catalyzed by **3** and **4** for the mono-addition product over 20 h.

Table S3 Results of the single addition product from the hydroamination reaction of crotonitrile (14a) catalyzed by complexes **3** and **4** over 2 h

ENTRY	SUBSTRATE	PRODUCT	CATALYST	TON[a] (Yield, %)	TOF[a] [h^{-1}]
1	**13a**	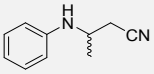 **15a**	**3**	28,6 ± 0,6	14,3 ± 0,3
2			**4**	40 ± 1	20,0 ± 0,7
3	**13b**	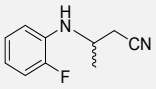 **15b**	**3**	4,9 ± 0,1	2,43 ± 0,03
4			**4**	9 ± 2	4 ± 1
5	**13c**	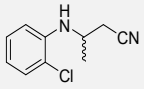 **15c**	**3**	2,6 ± 0,5	1,3 ± 0,3
6			**4**	1,3 ± 0,2	0,7 ± 0,1
7	**13d**	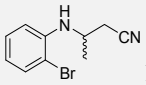 **15d**	**3**	2,0 ± 0,1	1,0 ± 0,1
8			**4**	3,9 ± 0,4	2,0 ± 0,2
9	**13e**	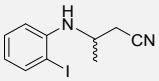 **15e**	**3**	0	0
10			**4**	0	0
11	**13f**	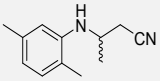 **15f**	**3**	1,1 ± 0,1	0,56 ± 0,04
12			**4**	4,8 ± 0,3	2,4 ± 0,2
13	**13g**	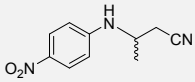 **15g**	**3**	0	0
14			**4**	0	0
15	**13h**	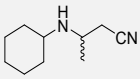 **15h**	**3**	36,4 ± 0,6	18,2 ± 0,3
16			**4**	23,9 ± 0,6	11,9 ± 0,3
17	**13i**	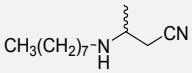 **15i**	**3**	56,1 ± 0,6	28,0 ± 0,3
18			**4**	28,2 ± 0,8	14,1 ± 0,4
19	**13j**	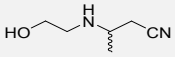 **15j**	**3**	18 ± 1	9,1 ± 0,7
20			**4**	6,8 ± 0,1	3,4 ± 0,1

a) TON and TOF are the average of three experiments under the same conditions.

Table S4 Results of the single addition product from the hydroamination reaction of crotonitrile (14a) catalyzed by complexes **3** and **4** over 20 h

ENTRY	SUBSTRATE	PRODUCT	CATALYST	TON[a] (Yield, %)	TOF[a] [h^{-1}]
1	13a	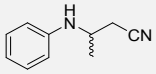 15a	3	48 ± 5	2,4 ± 0,3
2			4	29 ± 1	1,5 ± 0,1
3	13b	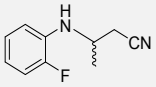 15b	3	11 ± 1	0,5 ± 0,1
4			4	7,1 ± 0,4	0,35 ± 0,02
5	13c	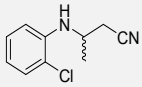 15c	3	3,5 ± 0,5	0,18 ± 0,02
6			4	1,8 ± 0,2	0,09 ± 0,01
7	13d	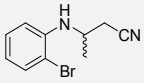 15d	3	1,3 ± 0,2	0,06 ± 0,01
8			4	2,0 ± 0,6	0,09 ± 0,03
9	13e	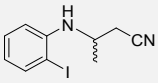 15e	3	0	0
10			4	0	0
11	13f	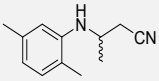 15f	3	15 ± 2	0,7 ± 0,1
12			4	10 ± 2	0,5 ± 0,1
13	13g	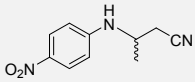 15g	3	0	0
14			4	0	0
15	13h	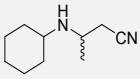 15h	3	43,5 ± 0,7	2,17 ± 0,04
16			4	26 ± 0,1	1,299 ± 0,004
17	13i	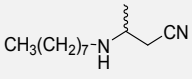 15i	3	64,4 ± 0,2	3,22 ± 0,01
18			4	33 ± 1	1,7 ± 0,1
19	13j	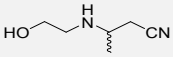 15j	3	12 ± 2	0,6 ± 0,1
20			4	5,8 ± 0,4	0,29 ± 0,02

a) TON and TOF are the average of three experiments under the same conditions.

Table S5 Formation of the double addition products from the hydroamination reaction of crotonitrile (14a) catalyzed by complexes **3** and **4** over 2 h

ENTRY	SUBSTRATE	PRODUCT	CATALYST	TON[a] (Yield, %)	TOF[a] [h^{-1}]
1	**13a**	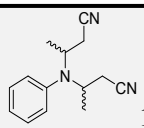 **15k**	**3**	0	0
2			**4**	0	0
3	**13b**	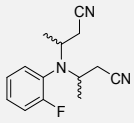 **15l**	**3**	0	0
4			**4**	0	0
5	**13c**	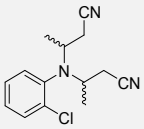 **15m**	**3**	0	0
6			**4**	0	0
7	**13d**	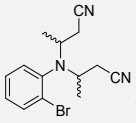 **15n**	**3**	0	0
8			**4**	0	0
9	**13e**	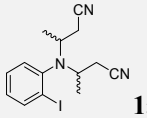 **15o**	**3**	0	0
10			**4**	0	0
11	**13f**	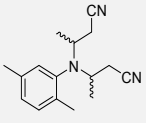 **15p**	**3**	0	0
12			**4**	0	0
13	**13g**	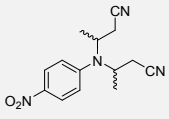 **15q**	**3**	0	0
14			**4**	0	0
15	**13h**	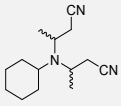 **15r**	**3**	0	0
16			**4**	0	0
17	**13i**	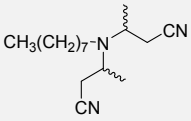 **15s**	**3**	3,5 ± 0,1	1,73 ± 0,03
18			**4**	0	0
19	**13j**	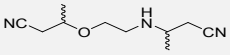 **15t**	**3**	0	0
20			**4**	0	0

a) TON and TOF are the average of three experiments under the same conditions.

Table S6 Formation of the double addition products from the hydroamination reaction of crotonitrile (14a) catalyzed by complexes **3** and **4** over 20 h

ENTRY	SUBSTRATE	PRODUCT	CATALYST	TON[a] (Yield, %)	TOF[a] [h^{-1}]
1	**13a**	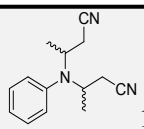 **15k**	**3**	0	0
2			**4**	0	0
3	**13b**	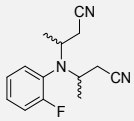 **15l**	**3**	0	0
4			**4**	0	0
5	**13c**	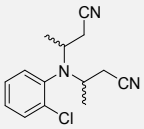 **15m**	**3**	0	0
6			**4**	0	0
7	**13d**	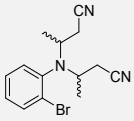 **15n**	**3**	0	0
8			**4**	0	0
9	**13e**	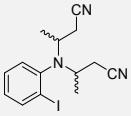 **15o**	**3**	0	0
10			**4**	0	0
11	**13f**	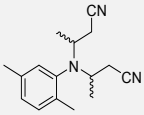 **15p**	**3**	0	0
12			**4**	0	0
13	**13g**	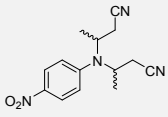 **15q**	**3**	0	0
14			**4**	0	0
15	**13h**	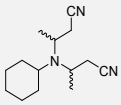 **15r**	**3**	0	0
16			**4**	0	0
17	**13i**	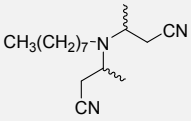 **15s**	**3**	3,6 ± 0,1	0,178 ± 0,005
18			**4**	0	0
19	**13j**	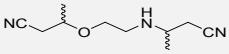 **15t**	**3**	0	0
20			**4**	0	0

a) TON and TOF are the average of three experiments under the same conditions.

Table S7 Results of the single addition product from the hydroamination reaction of methacrylonitrile (14b) catalyzed by complexes **3** and **4** over 2 h

ENTRY	SUBSTRATE	PRODUCT	CATALYST	TON[a] (Yield, %)	TOF[a] [h^{-1}]
1	**13a**	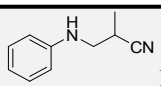 **16a**	**3**	21 ± 1	10,6 ± 0,7
2			**4**	35 ± 1	17,5 ± 0,7
3				38 ± 2 *	19 ± 1 *
4	**13b**	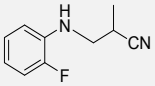 **16b**	**3**	5,2 ± 0,7	2,6 ± 0,4
5			**4**	7,8 ± 0,4	3,9 ± 0,2
6	**13c**	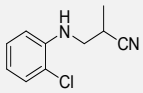 **16c**	**3**	3,2 ± 0,3	1,6 ± 0,2
7			**4**	0	0
8	**13d**	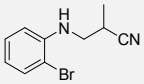 **16d**	**3**	2,4 ± 0,5	1,2 ± 0,2
9			**4**	3,2 ± 0,5	1,6 ± 0,3
10	**13e**	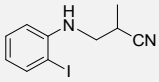 **16e**	**3**	0	0
11			**4**	0	0
12	**13f**	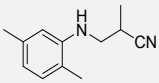 **16f**	**3**	7 ± 1	3,6 ± 0,5
13			**4**	0,6 ± 0,1	0,30 ± 0,03
14	**13g**	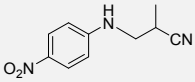 **16g**	**3**	0	0
15			**4**	0	0
16	**13h**	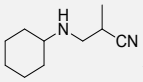 **16h**	**3**	39 ± 1	19,7 ± 0,6
17			**4**	22,7 ± 0,6	11,3 ± 0,3
18	**13i**	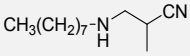 **16i**	**3**	34,6 ± 0,7	17,3 ± 0,3
19			**4**	12 ± 1	6,1 ± 0,5
20	**13j**	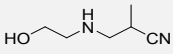 **16j**	**3**	14,6 ± 0,7	7,3 ± 0,4
21			**4**	0	0

a) TON and TOF are the average of three experiments under the same conditions. * In this experiment, 5 mmol of amine was used instead of 1 mmol

Table S8 Results of the single addition product from the hydroamination reaction of methacrylonitrile (14b) catalyzed by complexes **3** and **4** over 20 h

ENTRY	SUBSTRATE	PRODUCT	CATALYST	TON[a] (Yield, %)	TOF[a] [h^{-1}]
1	**13a**	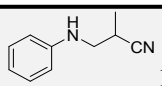 **16a**	**3**	41 ± 3	2,0 ± 0,1
2			**4**	28 ± 1	1,38 ± 0,05
3	**13b**	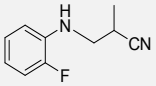 **16b**	**3**	12 ± 2	0,6 ± 0,1
4			**4**	10 ± 1	0,5 ± 0,1
5	**13c**	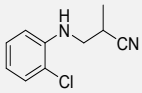 **16c**	**3**	3,3 ± 0,3	0,17 ± 0,02
6			**4**	3,4 ± 0,1	0,17 ± 0,01
7	**13d**	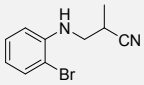 **16d**	**3**	1,9 ± 0,2	0,09 ± 0,01
8			**4**	2,2 ± 0,2	0,11 ± 0,01
9	**13e**	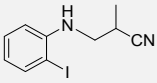 **16e**	**3**	0	0
10			**4**	0	0
11	**13f**	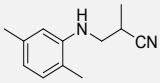 **16f**	**3**	15,5 ± 0,5	0,77 ± 0,02
12			**4**	14 ± 1	0,7 ± 0,1
13	**13g**	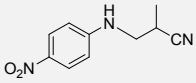 **16g**	**3**	0	0
14			**4**	0	0
15	**13h**	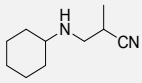 **16h**	**3**	41 ± 2	2,07 ± 0,09
16			**4**	25,4 ± 0,5	1,27 ± 0,03
17	**13i**	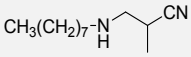 **16i**	**3**	36,4 ± 0,4	1,82 ± 0,02
18			**4**	16 ± 2	0,8 ± 0,1
19	**13j**	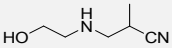 **16j**	**3**	10 ± 1	0,5 ± 0,1
20			**4**	1,5 ± 0,7	0.08 ± 0.04

a) TON and TOF are the average of three experiments under the same conditions.

Table S9 Formation of the double addition products from the hydroamination reaction of methacrylonitrile (14b) catalyzed by complexes **3** and **4** over 2 h

ENTRY	SUBSTRATE	PRODUCT	CATALYST	TON[a] (Yield, %)	TOF[a] [h^{-1}]
1	**13a**	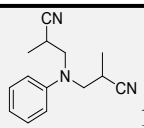 **16k**	**3**	4,7 ± 0,8	2,3 ± 0,4
2			**4**	0	0
3	**13b**	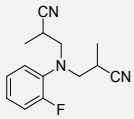 **16l**	**3**	0	0
4			**4**	0	0
5	**13c**	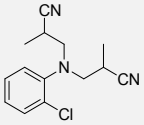 **16m**	**3**	0	0
6			**4**	0	0
7	**13d**	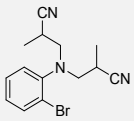 **16n**	**3**	0	0
8			**4**	0	0
9	**13e**	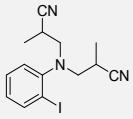 **16o**	**3**	0	0
10			**4**	0	0
11	**13f**	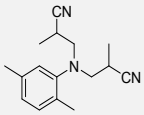 **16p**	**3**	0	0
12			**4**	0	0
13	**13g**	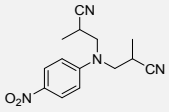 **16q**	**3**	0	0
14			**4**	0	0
15	**13h**	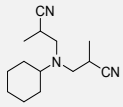 **16r**	**3**	0	0
16			**4**	0	0
17	**13i**	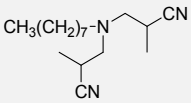 **16s**	**3**	2,1 ± 0,1	1,04 ± 0,06
18			**4**	0	0
19	**13j**	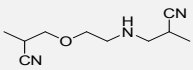 **16t**	**3**	0	0
20			**4**	0	0

a) TON and TOF are the average of three experiments under the same conditions.

Table S10 Formation of the double addition products from the hydroamination reaction of methacrylonitrile (14b) catalyzed by complexes **3** and **4** over 20 h

ENTRY	SUBSTRATE	PRODUCT	CATALYST	TON[a] (Yield, %)	TOF[a] [h^{-1}]
1	**13a**	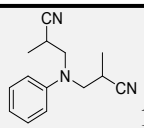 **16k**	**3**	5 ± 1	0,2 ± 0,1
2			**4**	0	0
3	**13b**	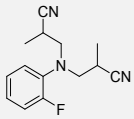 **16l**	**3**	0	0
4			**4**	0	0
5	**13c**	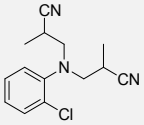 **16m**	**3**	0	0
6			**4**	0	0
7	**13d**	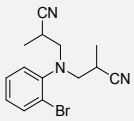 **16n**	**3**	0	0
8			**4**	0	0
9	**13e**	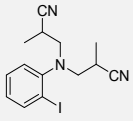 **16o**	**3**	0	0
10			**4**	0	0
11	**13f**	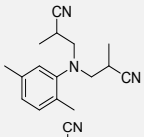 **16p**	**3**	0	0
12			**4**	0	0
13	**13g**	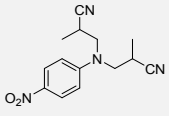 **16q**	**3**	0	0
14			**4**	0	0
15	**13h**	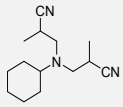 **16r**	**3**	0	0
16			**4**	0	0
17	**13i**	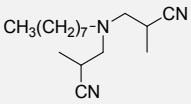 **16s**	**3**	2.0 ± 0,2	0,101 ± 0,01
18			**4**	0	0
19	**13j**	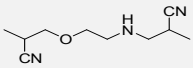 **16t**	**3**	0	0
20			**4**	0	0

a) TON and TOF are the average of three experiments under the same conditions.

Table S11 Testing the formation of the hydroamination product in the presence of either 14a or 14b and in the absence of catalyst over 2 h

ENTRY	SUBSTRATE	PRODUCT	NITRILE	TON[a] (Yield, %)	TOF[a] [h^{-1}]
1	13a	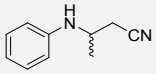 15a	14a	0	0
2			14b	0	0
3	13b	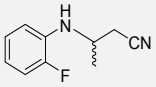 15b	14a	0	0
4			14b	0	0
5	13c	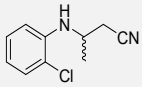 15c	14a	0	0
6			14b	0	0
7	13d	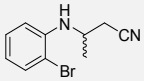 15d	14a	0	0
8			14b	0	0
9	13e	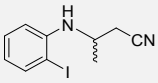 15e	14a	0	0
10			14b	0	0
11	13f	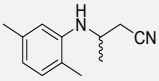 15f	14a	0	0
12			14b	0	0
13	13g	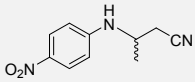 15g	14a	0	0
14			14b	0	0
15	13h	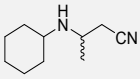 15h	14a	0	0
16			14b	0	0
17	13i	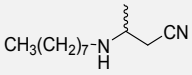 15i	14a	0	0
18			14b	0	0
19	13j	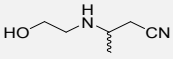 15j	14a	0	0
20			14b	0	0

a) TON and TOF are the average of three experiments under the same conditions.

References

(1) Sheldrick, G. *Acta Crystallographica Section A* **2008,** *64,* 112.
(2) Sheldrick, G. *Acta Crystallographica Section A* **2015,** *71,* 3.
(3) Dolomanov, O. V.; Bourhis, L. J.; Gildea, R. J.; Howard, J. A. K.; Puschmann, H. *J. Appl. Crystallogr.* **2009,** *42,* 339.